



# The construction and analysis of gene co-expression network of differentially expressed genes identifies potential biomarkers in thyroid cancer

Li Chai<sup>1,2#</sup>, Dongyan Han<sup>3#</sup>, Jin Li<sup>4</sup>, Zhongwei Lv<sup>1,2</sup>

<sup>1</sup>Department of Nuclear Medicine, The Affiliated Shanghai Tenth People's Hospital of Nanjing Medical University, Shanghai 200072, China;

<sup>2</sup>Department of Nuclear Medicine, <sup>3</sup>Department of Pathology, <sup>4</sup>Department of Geriatrics, Shanghai Tenth People's Hospital, Tongji University School of Medicine, Shanghai 200072, China

**Contributions:** (I) Conception and design: Z Lv; (II) Administrative support: J Li; (III) Provision of study materials or patients: L Chai; (IV) Collection and assembly of data: D Han; (V) Data analysis and interpretation: L Chai, D Han; (VI) Manuscript writing: All authors; (VII) Final approval of manuscript: All authors.

<sup>#</sup>These authors contributed equally to this study.

**Correspondence to:** Dr. Zhongwei Lv. Department of Nuclear Medicine, The Affiliated Shanghai Tenth People's Hospital of Nanjing Medical University, Shanghai 200072, China; Department of Nuclear Medicine, Shanghai Tenth People's Hospital, Tongji University School of Medicine, 301 Yanchang Road, Shanghai 200072, China. Email: doctorcl@163.com.

**Background:** The incidence and mortality of thyroid cancer has been increasing steadily in the United States. However, the molecular pathogenesis of thyroid cancer is not fully characterized.

**Methods:** The R package of DESeq2 was applied to detect differentially expressed genes (DEGs) between 57 paired thyroid cancer and noncancerous tissues using RNA sequencing data from The Cancer Genome Atlas database. Weighted gene co-expression network analysis was used to construct co-expression modules and study the relationship between co-expression modules and clinical traits. Gene ontology (GO) enrichment analysis was performed on these genes from interested co-expression modules.

**Results:** A cohort of 750 up-regulated and 296 down-regulated genes were identified in thyroid cancer. The weighted gene co-expression network analysis identified 5 gene co-expression modules. Two modules were significantly associated with patients' age, cancer stage and multifocality. *SERPINA1* and *MRO* were their hub genes respectively.

**Conclusions:** The bioinformatics study for those co-expression modules and hub genes paves the way for the development of molecular biomarkers in thyroid cancer.

**Keywords:** Thyroid cancer; differentially expressed genes (DEGs); gene ontology (GO); weighted correlation network analysis

Submitted Jul 30, 2018. Accepted for publication Sep 17, 2018.

doi: 10.21037/tcr.2018.09.12

**View this article at:** <http://dx.doi.org/10.21037/tcr.2018.09.12>

## Introduction

Over the past 4 decades, the incidence of thyroid cancer has been increasing steadily in United States, with 14.42 cases per 100,000 persons per year in 2010–2013 (1). The most common histologic types were papillary thyroid cancer (PTC) (84%) and follicular thyroid cancer (11%). Thyroid cancer mortality rate rose by 1.1% annually from

0.40 per 100,000 person-years in 1994–1997 and to 0.46 per 100,000 person-years in 2010–2013 (1). Therefore, characterization of the molecular pathogenesis of thyroid cancer is critical to identifying key biomarkers and effective therapeutic targets for the disease.

Numerous studies have been conducted to characterize the genomic and transcriptomic landscapes of thyroid

cancer. The Cancer Genome Atlas (TCGA) applied MutSig to 496 paired tumor/normal samples and found many frequently mutated driver genes in thyroid cancer, such as *BRAF*, *NRAS*, *HRAS*, *EIF1AX* and *KRAS* (2). The study confirmed that PTCs are driven primarily by mutations in one of two cancer-associated genes: *BRAF(V600E)* or *RAS*. Yoo *et al.* classified thyroid tumors into three molecular subtypes, including *BRAF*-like, *RAS*-like, and Non-*BRAF*-Non-*RAS* based on gene expression profiles. *BRAF*-like patients showed higher frequency of lymph node metastasis or extrathyroidal extension, while patients in the *RAS*-like group or Non-*BRAF*-Non-*RAS* group showed less or no lymph node metastasis or extrathyroidal extension (3). Costa *et al.* identified a new gene fusion *WNK1-B4GALNT3* that was correlated with *B4GALNT3* overexpression in a cohort of 18 PTC patients using RNA-Sequencing (4).

The weighted correlation network analysis (WGCNA) package comprises a series of R functions to perform a variety of weighted correlation network analyses. WGCNA detects co-expression modules of highly correlated genes and associates interested modules with clinical traits, providing insights into signaling networks that may be responsible for phenotypic traits (5). In this study, we performed a genome-wide investigation of differentially expressed genes (DEGs) in 57 pairs of thyroid cancer and normal thyroid tissues. WGCNA was applied to build co-expression modules using the expression data of DEGs in thyroid cancer. Module-trait associations were analyzed using the correlation between the module eigengene and clinical traits. Gene ontology (GO) enrichment analysis was performed on the genes and the hub genes were identified in the modules of interest (6). These findings may be of importance in evaluating the malignant potential and clinical outcomes of thyroid cancer patients.

## Methods

### *DEG and principal component analyses*

Among 568 thyroid cancer samples in TCGA, only 57 samples had RNA-sequencing expression data of paired normal thyroid tissues. Therefore, raw count data of 57 thyroid cancer and paired normal thyroid samples were retrieved from the TCGA database at the Broad Institute for DEGs analysis (7) (<http://firebrowse.org/?cohort=THCA>). In order to further validate DEGs, we obtained RNA-seq expression data of 8 pairs of thyroid cancer and normal thyroid tissues from Gene Expression Omnibus (GEO) (GSE63511) (8). The R package of DESeq2 was used to

characterize the expression profiles in 57 thyroid cancer and paired normal tissues (9). If genes showed false discovery rates (FDR) smaller than 0.05 and absolute log<sub>2</sub>fold-changes greater than 2, they were considered as DEGs. Next, principal component analysis (PCA) was conducted to evaluate whether DEGs could distinguish thyroid cancer from normal tissues.

### *GO enrichment analysis*

To analyze the functional enrichment of DEGs and genes in co-expression modules, GO (6)-enrichment analysis was performed for all the DEGs and genes in co-expression modules with the online tool of GO (<http://geneontology.org/>). If the cutoff of FDR adjusted P value was smaller than 0.05, the enrichment of GO terms was considered to be significant.

### *Construction of co-expression network in thyroid cancer*

Soft-thresholding power values were screened out in the construction of co-expression modules by the WGCNA algorithm (5). The gradient method was applied to evaluate the scale-free fit index and the mean connectivity degree of different co-expression modules with power values ranging from 1 to 20. The optimal power value was determined when the scale-free fit index was above 0.8, and then the construction of co-expression modules was performed by the WGCNA algorithm in R3.2.0. The minimum number of genes was set as 10 to ensure the high reliability of the results. The corresponding genetic information of co-expression modules was also extracted.

### *Characterization of module-trait relationships in thyroid cancer*

Module-trait associations were analyzed using the correlation between the module eigengenes and clinical phenotypes, which enabled the identification of co-expression modules with significant correlation with the phenotype. For each expression profile, gene significance (GS) was calculated as the absolute value of the correlation between expression profile and each trait; module membership (MM) was defined as the correlation of expression profile and each module eigengene (10). Using the GS and MM measures, genes that have a high significance for each trait as well as high MM in interesting modules could be identified. The intramodular connectivity was computed for each gene by

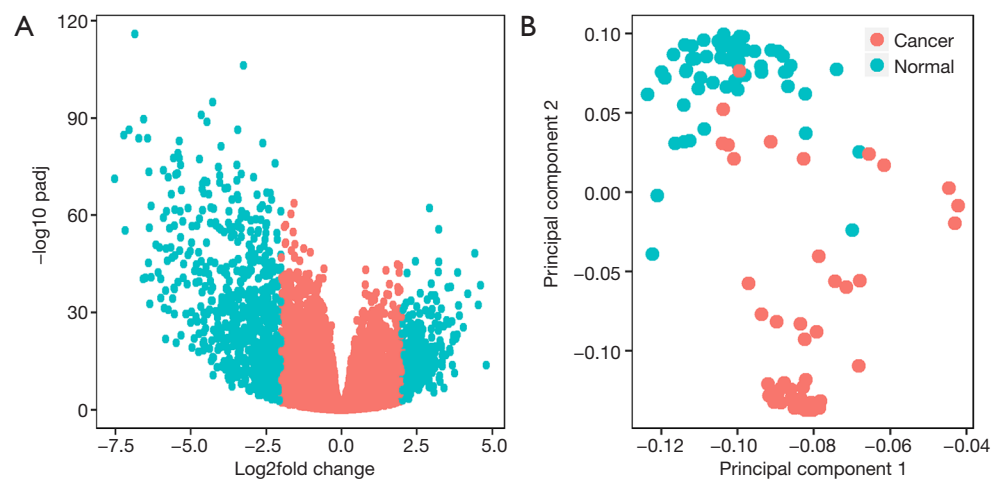


**Figure 1** Differentially expressed gene analysis in thyroid cancer. (A) The volcano plot shows the distribution of DEGs (cyan dots) in the expression analysis (all DEGs shown in cyan dots had absolute log<sub>2</sub>fold change >2 and FDR <0.05); (B) PCA analysis of the 57 paired thyroid cancer and normal samples using 1,046 DEGs. Red and blue dots denote thyroid cancer and normal samples respectively. Each dot represents the expression values of the DEGs that were summarized at the first two principal component coordinates. DEGs, differentially expressed genes; FDR, false discovery rates.

summing the connection strengths with other module genes and dividing this number by the maximum intramodular connectivity. The genes with maximum intramodular connectivity were regarded as intramodular hub genes (11). The interested modules and hub genes were visualized by Integrative Visual Analysis Tool for Biological Networks and Pathways (VisANT) (12) software.

## Results

### DEGs analysis

The 57 thyroid cancer samples comprise 48 papillary, 6 follicular and 3 tall cell thyroid cancer samples. Twenty nine cancer samples had BRAFV600E mutations, while 28 samples were wild-type. Six and 51 cancer samples were RAS-mutant or wild-type respectively. Raw count data of thyroid cancer and normal samples were obtained from TCGA. DEGs were determined between 57 pairs of thyroid cancer and normal tissues with DESeq2 package in R. Overall, DESeq2 found 750 up-regulated and 296 down-regulated genes (Figure 1A). *ARHGAP36*, *TMPRSS6*, *DMBX1*, *LOC400794*, *GABRB2*, *ZCCHC12*, *KLK6*, *KLK10*, *CST2* and *GRM4* were the top-ranking up-regulated genes, while *CHGA*, *SLC6A15*, *IHH*, *TSPAN19*, *PMP2*, *KCNA1*, *PCDH11X*, *TFF3*, *GPR142* and *C6orf176* were the top-ranking down-regulated genes in thyroid cancer (Table 1). In order to confirm the

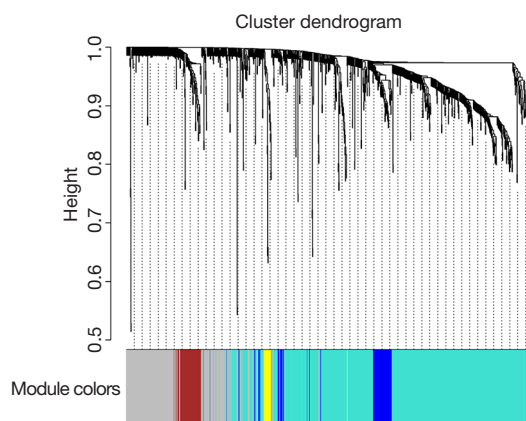
DEGs in thyroid cancer, we obtained RNA-seq data of 8 pairs of thyroid cancer and normal thyroid tissues from GEO. 77 genes were determined as DEGs by DESeq2, 64.81% (35/54) up-regulated and 52.17% (12/23) down-regulated genes were overlapped with the DEGs obtained from 57 pairs of thyroid cancer and normal counterparts (Figure S1). Next, PCA was conducted to assess whether DEGs could distinguish thyroid cancer from normal tissues. Cancer and normal tissues were aggregated to the lower and upper sides respectively, demonstrating that DEGs were able to classify the samples into two distinct subsets (Figure 1B).

### GO term enrichment analysis

The enrichment of GO terms was analyzed for 750 up-regulated and 296 down-regulated genes on the home page of GO. GO term enrichment analysis showed down-regulated genes were significantly enriched in 136 biological processes, up-regulated genes in 281 biological processes (FDR adjusted P value <0.05). The main GO biological process terms for down-regulated genes showed a wide variety of functional processes ranging from cellular developmental process, cell differentiation, single-multicellular organismal process, cell development and regulation of system process. While the primary GO terms for up-regulated genes were related to various cellular processes, such as negative regulation of endopeptidase activity, cell-cell adhesion, epidermis

**Table 1** The top 10 down-regulated and up-regulated genes in thyroid cancer

Gene	Fold change	P value	FDR-adjusted P value
Down-regulated			
CHGA	4.80	$1.55 \times 10^{-15}$	$1.48 \times 10^{-14}$
SLC6A15	4.61	$5.82 \times 10^{-41}$	$4.16 \times 10^{-39}$
IHH	4.54	$1.08 \times 10^{-34}$	$5.03 \times 10^{-33}$
TSPAN19	4.42	$4.05 \times 10^{-51}$	$5.56 \times 10^{-49}$
PMP2	4.18	$2.46 \times 10^{-38}$	$1.46 \times 10^{-36}$
KCNA1	4.05	$1.17 \times 10^{-27}$	$3.24 \times 10^{-26}$
PCDH11X	3.91	$2.43 \times 10^{-31}$	$8.81 \times 10^{-30}$
TFF3	3.88	$1.24 \times 10^{-34}$	$5.71 \times 10^{-33}$
GPR142	3.86	$4.25 \times 10^{-45}$	$4.04 \times 10^{-43}$
C6orf176	3.79	$4.10 \times 10^{-24}$	$8.52 \times 10^{-23}$
Up-regulated			
ARHGAP36	-7.53	$8.54 \times 10^{-75}$	$5.22 \times 10^{-72}$
TMPRSS6	-7.22	$1.15 \times 10^{-88}$	$2.42 \times 10^{-85}$
DMBX1	-7.17	$2.47 \times 10^{-58}$	$4.72 \times 10^{-56}$
LOC400794	-7.05	$2.04 \times 10^{-90}$	$4.83 \times 10^{-87}$
GABRB2	-6.86	$6.29 \times 10^{-121}$	$1.19 \times 10^{-116}$
ZCCHC12	-6.72	$1.34 \times 10^{-87}$	$2.31 \times 10^{-84}$
KLK6	-6.58	$4.42 \times 10^{-43}$	$3.58 \times 10^{-41}$
KLK10	-6.57	$6.60 \times 10^{-94}$	$2.50 \times 10^{-90}$
CST2	-6.51	$2.79 \times 10^{-43}$	$2.31 \times 10^{-41}$
GRM4	-6.43	$1.23 \times 10^{-87}$	$2.31 \times 10^{-84}$

**Figure 2** Clustering dendrograms of genes found 5 co-expression modules shown in different colors.

development, extracellular matrix organization, regulation of protein phosphorylation, regulation of signal transduction, regulation of cell proliferation and a variety of metabolic processes.

### Construction of co-expression modules in thyroid cancer

Among the 568 thyroid cancer samples in TCGA, 501 had both RNA-sequencing expression and clinical traits data. Therefore, expression values of 1,046 genes in the 501 samples of thyroid cancer were used to construct the co-expression modules by the WGCNA package. One of the most important parameters was the soft-thresholding power value, which mainly affected the scale-free fit index and the average connectivity degree of co-expression modules. Firstly, the power value was screened out (*Figure S2*). When the power value was equal to seven, the scale-free fit index was larger than 0.8 and the mean connectivity degree was higher. Therefore, the soft-thresholding power value used to construct co-expression modules and the WGCNA identified five distinct gene co-expression modules which are shown in different colors (*Figure 2*). These numbers of genes in the five modules differed largely, with 608, 293, 70, 57 and 19 genes for the turquoise, grey, blue, brown and yellow modules respectively (*Figure 2*).

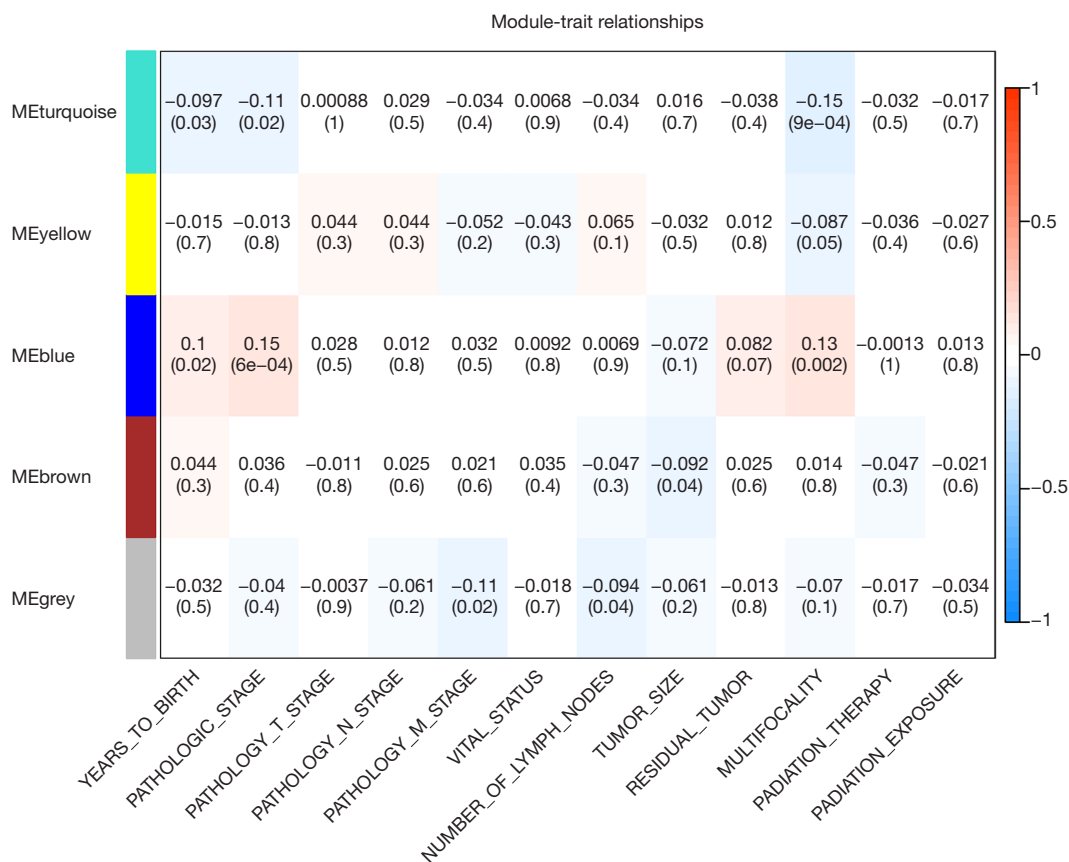


**Figure 3** The co-expression module-trait associations. Each row corresponds to a module eigengene, column to a trait. Each cell contains the corresponding correlation co-efficient and P value. The right red-to-blue bar shows the negative (blue) to positive (red) correlations between co-expression modules and clinical traits.

**Module-trait association analysis in thyroid cancer**

The clinical traits data were obtained from the TCGA database. Module-trait associations were analyzed with the correlation between module eigengene and clinical traits. As showed in the *Figure 3*, the turquoise module was negatively correlated with patients’ age, cancer stage and multifocality (P value <0.05 for all cases, *Figures 2 and 3*). In contrast, the blue module was significantly positively associated with patients’ age, cancer stage and multifocality (P value <0.05 for all cases, *Figures 2 and 3*). The brown module was negatively correlated with tumor size (P value =0.04, *Figures 2 and 3*). Then, we plotted scatterplots of GS for patients’ age, cancer stage, multifocality and tumor size *vs.* MM in the blue, turquoise and brown modules. The GS for patients’ age, cancer stage and multifocality was positively correlated with MM in the blue and turquoise modules (P value <0.05 for all cases, *Figure 4*). However, the GS for

tumor size showed non-significant correlation with MM in the brown module (P=0.81, *Figure S3*).

**Functional enrichment analysis of genes in the interested modules**

GO enrichment analysis was performed on the genes in the turquoise, blue and brown modules. There was large difference in the biological processes in which the three modules were enriched. Genes in turquoise module were significantly over-represented in 171 GO terms (FDR adjusted P value <0.05), such as cell migration (GO:0016477), regulation of cell proliferation (GO:0042127), regulation of cell differentiation (GO:0045595), regulation of cellular protein metabolic process (GO:0032268), signal transduction (GO:0007165). While genes in the turquoise module were significantly

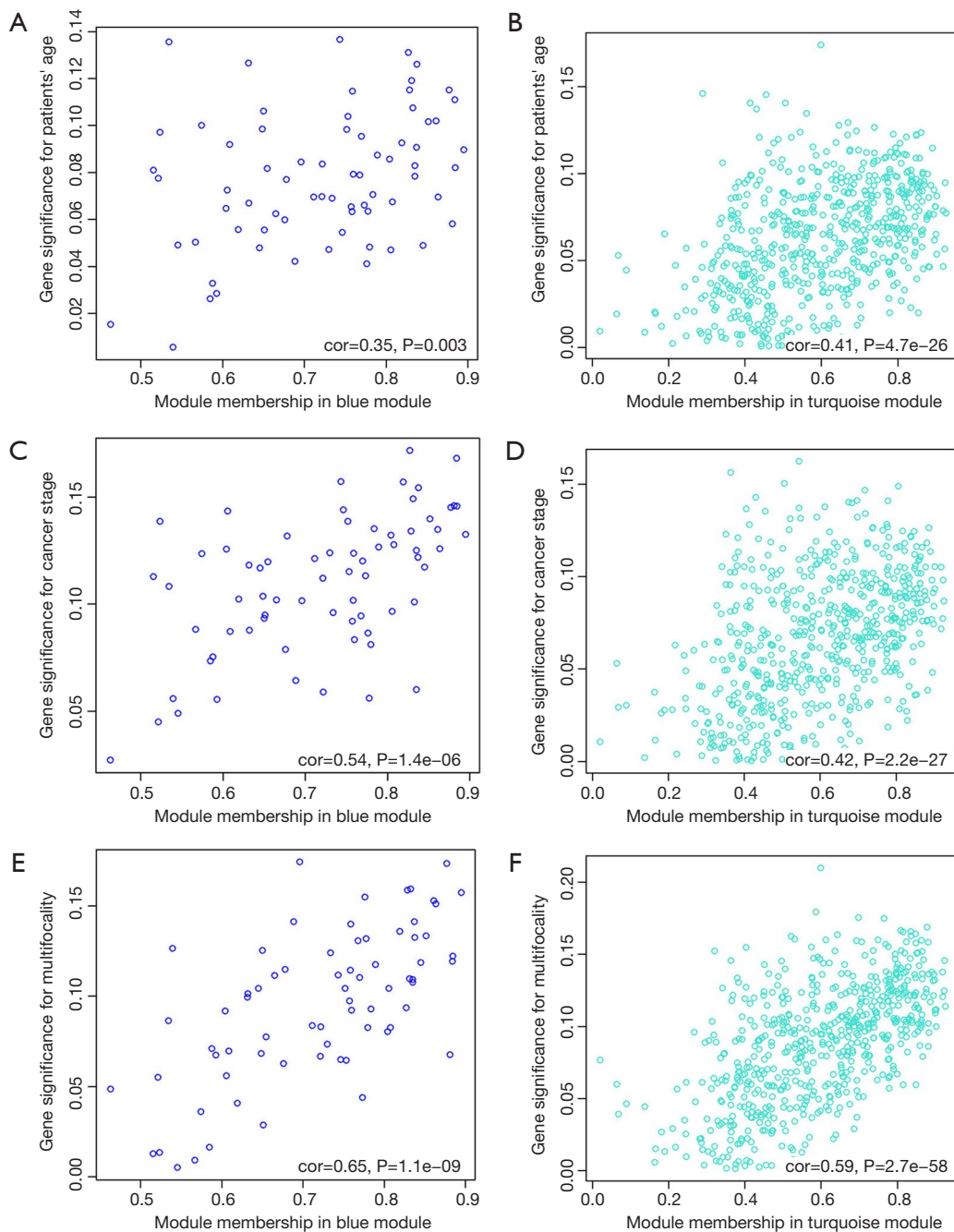


**Figure 4** The correlations between GS of clinical traits and MM in the blue and turquoise modules of thyroid cancer. Scatterplots of GS for patients' age *vs.* MM in the blue (A) and turquoise (B) modules. Scatterplots of GS for cancer stage *vs.* MM in the blue (C) and turquoise (D) modules. Scatterplots of GS for multifocality *vs.* MM in the blue (E) and turquoise (F) modules. GS and MM refer to gene significance and module membership respectively. GS, gene significance; MM, module membership.

under-represented in 42 GO terms, such as gene expression (GO:0010467), DNA repair (GO:0006281), DNA metabolic process (GO:0006259) and cellular response

to DNA damage stimulus (GO:0006974). However, no significant enrichment of GO terms was found for the genes in the blue and brown modules.

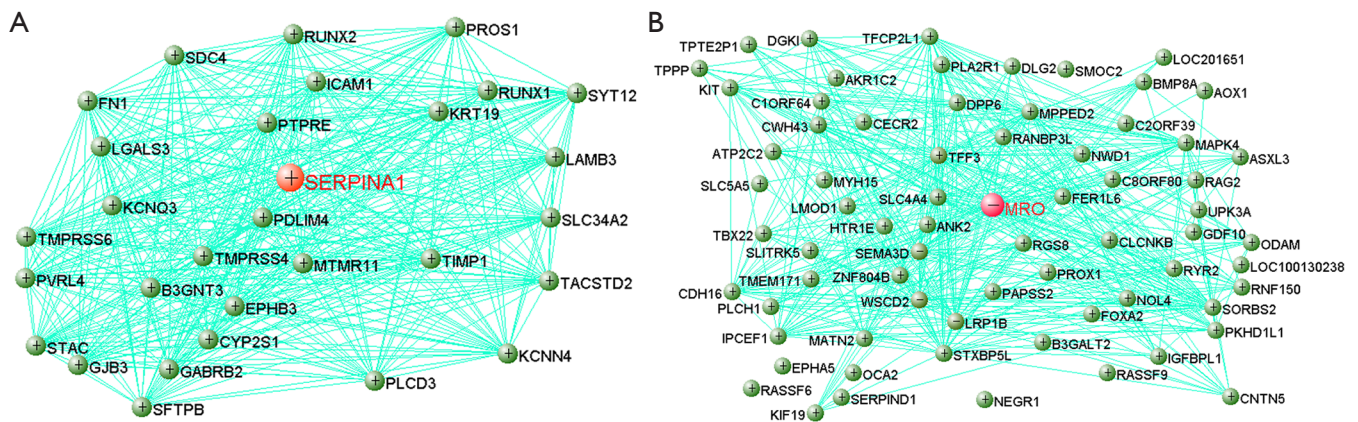


**Figure 5** Visualization of the turquoise (A) and blue (B) modules and hub genes. Notably, the top 30 DEGs which have maximum connections with other genes were shown in the turquoise module. The genes with weighted cutoff value of  $\geq 0.05$  are shown. Each node represents a gene. The hub genes were shown in red in the modules. DEGs, differentially expressed genes.

### Visualization of the interested modules and hub genes

The modules were constructed using the VisANT software. The genes with largest intramodular connectivity were considered as intramodular hub genes. The hub genes in the turquoise and blue modules were bold with red in *Figure 5*. *SERPINA1* and *MRO* were the hub genes in the turquoise and blue modules respectively (*Figure 5*).

### Discussion

RNA-seq analyses have previously been used to predict therapeutic biomarkers and to identify gene expression patterns associated with clinical traits in thyroid cancer (13,14). This study presented a large number of DEGs between 57 pairs of thyroid cancer and normal tissues. By comparing the DEGs to the tumor associated gene and tumor suppressor databases (15), five known oncogenes were up-regulated, including *ELF3*, *HMG2*, *LCN2*, *MET* and *RUNX2*; by contrast, 10 TSGs were found down-regulated, including *EGR2*, *FOXA2*, *GPC3*, *IGFBP1*, *LRP1B*, *MT1G*, *NR4A3*, *PROX1*, *TMEFF2* and *WNT11*. Additionally, some new DEGs were discovered, such as *ARHGAP36*, *TMPRSS6*, *DMBX1*, *CHGA* and *SLC6A15*, which have not been reported previously and their functions remain unknown in thyroid cancer.

WGCNA is a method frequently used to explore the co-expression modules of highly correlated genes. Genes in the same module were considered to be related with each other in function. Therefore, the analysis allowing for identification of biologically-relevant modules and

hub genes that may eventually serve as biomarkers for detection or treatment (5). In this study, a total of five co-expression modules were constructed by the 1,046 genes from the 57 pairs of thyroid cancer and normal samples by the WGCNA method. We identified the blue and turquoise co-expression modules that relate to clinical traits (patient's age, cancer stage and multifocality, *Figures 2-4*). The result of functional enrichment analysis showed that the turquoise module was found to be mainly enriched in cellular processes associated with cell migration, regulation of cell proliferation, regulation of cell differentiation, and regulation of cellular protein metabolic process. While genes in the blue module were not significantly enriched in any GO terms. Therefore, we speculate that turquoise module is the most important module in the cancer stage and multifocality of thyroid cancer.

The turquoise and blue co-expression modules were constructed by the VisANT software and the hub genes *SERPINA1* and *MRO* were identified (*Figure 5*). The *SERPINA1*, also known as  $\alpha 1$ -AntiTrypsin, is a protease inhibitor that can act on a variety of targets such as serine proteases. It has been demonstrated that *SERPINA1* expression can be stimulated by E2 in MCF-7 cells, and a high expression of this protein inhibits colony formation (16). *SERPINA1* is up-regulated in colorectal cancer (17), glioma (18), cutaneous squamous cell carcinoma (19) and thyroid cancer (20). *SERPINA1* has been proposed as a biomarker for various cancers, such as papillary thyroid carcinoma (20), lung cancer (21) and breast carcinoma (22-24). The high expression of *SERPINA1* indicates a poor prognosis

of high-grade glioma (18) but a favorable clinical outcome in breast cancer patients (25). The hub gene of the blue module is *MRO*, which is down-regulated in lung cancer cell lines (26). The hub genes in the turquoise and blue modules are either oncogenes or anti-oncogenes. Therefore, we speculate that the hub genes are critical in the cancer stage and multifocality of thyroid cancer.

## Conclusions

Taken together, the turquoise module was regarded as the most critical module in the cancer stage and multifocality of thyroid cancer. More importantly, the hub gene *SERPINA1* may function as a potential biomarker for thyroid cancer, which also needs much further research.

## Acknowledgments

*Funding:* None.

## Footnote

*Conflicts of Interest:* All authors have completed the ICMJE uniform disclosure form (available at <http://dx.doi.org/10.21037/tcr.2018.09.12>). The authors have no conflicts of interest to declare.

*Ethical Statement:* The authors are accountable for all aspects of the work in ensuring that questions related to the accuracy or integrity of any part of the work are appropriately investigated and resolved. The study was conducted in accordance with the Declaration of Helsinki (as revised in 2013). Institutional ethical approval and informed consent were waived.

*Open Access Statement:* This is an Open Access article distributed in accordance with the Creative Commons Attribution-NonCommercial-NoDerivs 4.0 International License (CC BY-NC-ND 4.0), which permits the non-commercial replication and distribution of the article with the strict proviso that no changes or edits are made and the original work is properly cited (including links to both the formal publication through the relevant DOI and the license). See: <https://creativecommons.org/licenses/by-nc-nd/4.0/>.

## References

1. Lim H, Devesa SS, Sosa JA, et al. Trends in thyroid cancer incidence and mortality in the United States, 1974-2013. *JAMA* 2017;317:1338-48.
2. Cancer Genome Atlas Research Network. Integrated Genomic Characterization of Papillary Thyroid Carcinoma. *Cell* 2014;159:676-90.
3. Yoo SK, Lee S, Kim SJ, et al. Comprehensive Analysis of the Transcriptional and Mutational Landscape of Follicular and Papillary Thyroid Cancers. *PLoS Genet* 2016;12:e1006239.
4. Costa V, Esposito R, Ziviello C, et al. New somatic mutations and gene fusion in papillary thyroid carcinoma. *Oncotarget* 2015;6:11242-51.
5. Langfelder P, Horvath S. WGCNA: an R package for weighted correlation network analysis. *BMC Bioinformatics* 2008;9:559.
6. Ashburner M, Ball CA, Blake JA, et al. Gene ontology: tool for the unification of biology. The Gene Ontology Consortium. *Nat Genet* 2000;25:25-9.
7. Cancer Genome Atlas Research Network, Weinstein JN, Collisson EA, et al. The Cancer Genome Atlas Pan-Cancer analysis project. *Nat Genet* 2013;45:1113-20.
8. Riesco-Eizaguirre G, Wert-Lamas L, Perales-Paton J, et al. The miR-146b-3p/PAX8/NIS regulatory circuit modulates the differentiation phenotype and function of thyroid cells during carcinogenesis. *Cancer Res* 2015;75:4119-30.
9. Love MI, Huber W, Anders S. Moderated estimation of fold change and dispersion for RNA-Seq data with DESeq2. *Genome Biol* 2014;15:550.
10. Shi K, Bing ZT, Cao GQ, et al. Identify the signature genes for diagnose of uveal melanoma by weight gene co-expression network analysis. *Int J Ophthalmol* 2015;8:269-74.
11. Wisniewski N, Cadeiras M, Bondar G, et al. Weighted Gene Coexpression Network Analysis (WGCNA) Modeling of Multiorgan Dysfunction Syndrome after Mechanical Circulatory Support Therapy. *J Hear Lung Transplant* 2018;32:S223.
12. Hu Z, Mellor J, Wu J, et al. VisANT: An online visualization and analysis tool for biological interaction data. *BMC Bioinformatics* 2004;5:17.
13. Qiu J, Zhang W, Xia Q, et al. RNA sequencing identifies crucial genes in papillary thyroid carcinoma (PTC) progression. *Exp Mol Pathol* 2016;100:151-9.
14. Baldan F, Mio C, Allegri L, et al. Identification of tumorigenesis-related mRNAs associated with RNA-binding protein HuR in thyroid cancer cells. *Oncotarget* 2016;7:63388-407.

15. Zhao M, Sun J, Zhao Z. TSGene: A web resource for tumor suppressor genes. *Nucleic Acids Res* 2013;41:D970-6.
16. Finlay TH, Tamir S, Kadner SS, et al. alpha 1-Antitrypsin- and anchorage-independent growth of MCF-7 breast cancer cells. *Endocrinology* 1993;133:996-1002.
17. Pérez-Holanda S, Blanco I, Menéndez M, et al. Serum concentration of alpha-1 antitrypsin is significantly higher in colorectal cancer patients than in healthy controls. *BMC Cancer* 2014;14:355.
18. Ookawa S, Wanibuchi M, Kataoka-Sasaki Y, et al. Digital Polymerase Chain Reaction Quantification of SERPINA1 Predicts Prognosis in High-Grade Glioma. *World Neurosurg* 2018;111:e783-9.
19. Farshchian M, Kivisaari A, Ala-Aho R, et al. Serpin peptidase inhibitor clade a member 1 (SerpinA1) is a novel biomarker for progression of cutaneous squamous cell carcinoma. *Am J Pathol* 2011;179:1110-9.
20. Vierlinger K, Mansfeld MH, Koperek O, et al. Identification of SERPINA1 as single marker for papillary thyroid carcinoma through microarray meta analysis and quantification of its discriminatory power in independent validation. *BMC Med Genomics* 2011;4:30.
21. Topic A, Ljubic M, Nikolic A, et al. Alpha-1-antitrypsin phenotypes and neutrophil elastase gene promoter polymorphisms in lung cancer. *Pathol Oncol Res* 2011;17:75-80.
22. López-Árias E, Aguilar-Lemarroy A, Felipe Jave-Suárez L, et al. Alpha 1-antitrypsin: A novel tumor-associated antigen identified in patients with early-stage breast cancer. *Electrophoresis* 2012;33:2130-7.
23. Doustjalali SR, Yusof R, Yip CH, et al. Aberrant expression of acute-phase reactant proteins in sera and breast lesions of patients with malignant and benign breast tumors. *Electrophoresis* 2004;25:2392-401.
24. Abbott KL, Aoki K, Lim JM, et al. Targeted glycoproteomic identification of biomarkers for human breast carcinoma. *J Proteome Res* 2008;7:1470-80.
25. Chan HJ, Li H, Liu Z, et al. SERPINA1 is a direct estrogen receptor target gene and a predictor of survival in breast cancer patients. *Oncotarget* 2015;6:25815-27.
26. Yanaihara N, Kohno T, Takakura S, et al. Physical and Transcriptional Map of a 311-kb Segment of Chromosome 18q21, a Candidate Lung Tumor Suppressor Locus. *Genomics* 2001;72:169-79.

**Cite this article as:** Chai L, Han D, Li J, Lv Z. The construction and analysis of gene co-expression network of differentially expressed genes identifies potential biomarkers in thyroid cancer. *Transl Cancer Res* 2018;7(5):1235-1243. doi: 10.21037/tcr.2018.09.12

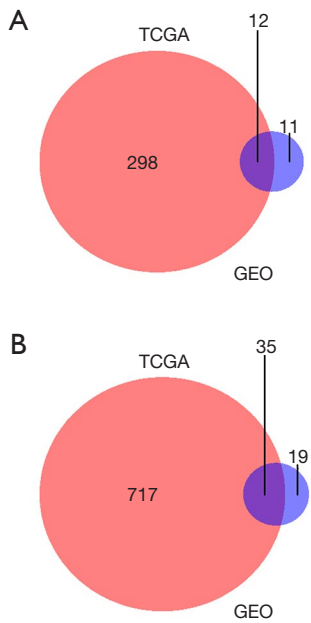


**Figure S1** The overlap of DEGs between 57 (TCGA) and 8 (GEO) pairs of thyroid cancer and normal thyroid tissues. (A) The overlap of down-regulated genes between the two datasets; (B) the overlap of up-regulated genes between the two datasets. DEGs, differentially expressed genes.

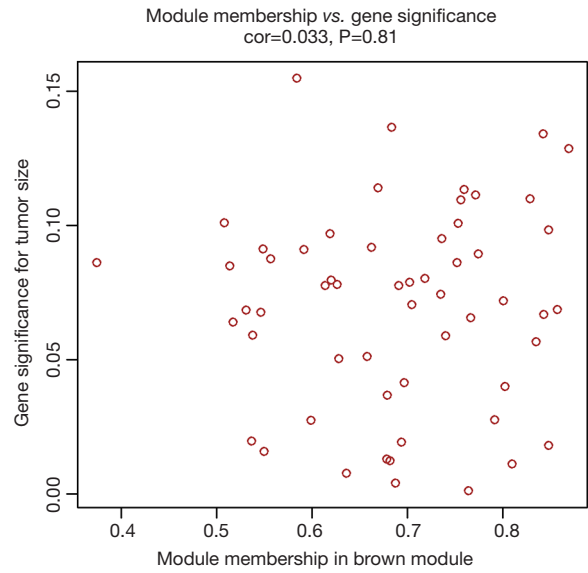


**Figure S3** A scatterplot of GS for tumor size *vs.* MM in the brown module. GS, gene significance; MM, module membership.

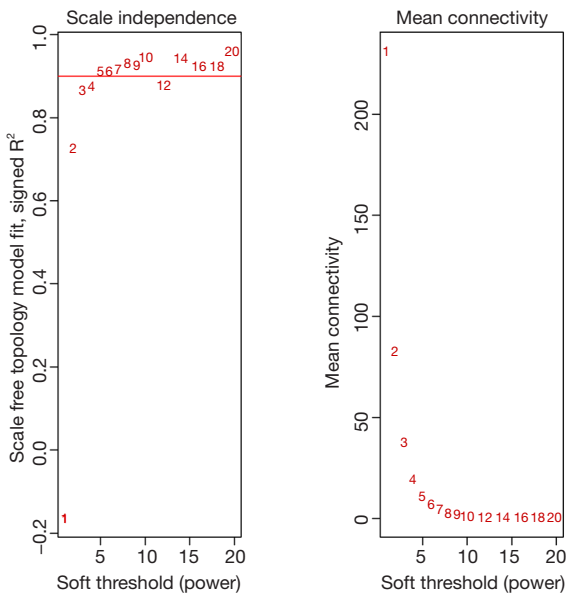


**Figure S2** Analysis of network topology for various soft-thresholding powers. The left panel shows the scale-free fit index (y-axis) as a function of the soft-thresholding power (x-axis). The right panel displays the mean connectivity (degree, y-axis) as a function of the soft-thresholding power (x-axis).